

# Electrocardiographic characteristics of significant factors of detected atrial fibrillation using WEMS

Min Soo Kim<sup>1)</sup>, Yoon Nyun Kim<sup>2)</sup>, Young Chang Cho<sup>3)\*</sup>

**Abstract** The wireless electrocardiographic monitoring system(WDMS) is designed to be long term monitoring for the early detection of cardiac disorders. The current version of the WDMS can identify two types of cardiac rhythms in real-time, such as atrial fibrillation(AF) and normal sinus rhythm(NSR), which are very important to track cardiac-rhythm disorders. In this study, we proposed the analysis method to discriminate the characteristics statistically evaluated in both time and frequency domains between AF and NSR using various parameters in the heart rate variability(HRV). And we applied various ECG detection methods (e.g., difference operation method) and compared the results with those of the discrete wavelet transform(DWT) method. From the statistically results, we found that the parameters such as STD RR, STD HR, RMSSD, NN50, pNN50, RR Trian, and TNN( $p < 0.05$ ) are significantly different between the AF and NSR patients in time domain. On the other hand, the frequency domain analysis results showed a significant difference in VLF power( $\text{ms}^2$ ), LF power( $\text{ms}^2$ ), HF power( $\text{ms}^2$ ), VLF(%), LF(%), and HF(%). In particular, the parameters such as STD RR, RMSSD, NN50, pNN50, VLF power, LF power and HF power were considered as the most useful parameters in both AF and NSR patient groups. Our proposed method can be efficiently applied to early detection of abnormal conditions and prevent the such abnormal from becoming serious.

**Key Words** : Wireless electrocardiographic monitoring system(WEMS), Wavelet transform (DWT), Arrhythmias, Atrial fibrillation(AF), Heart rate variability(HRV)

## 1. Introduction

AF is the most common cardiac arrhythmia, affecting nearly 1% of the population. Its prevalence increases with age; although relatively infrequent in those younger than 40 years, it occurs in up to 5% of those older than 80 years. Most people with a normal sinus rhythm(NSR) have a resting heart rate

of between 60 and 100 beats per min. In AF patients, the atrium contracts rapidly and irregularly at rates between 400 and 800 beats per min[1]. The major shortcomings of the standard 24-h Holter recording include poor detection rates of transient arrhythmic events. The current 24-h Holter monitors have been shown to miss many arrhythmias that may occur infrequently or under specific circumstances[2]. Senatore et al.[3] studied the incidence of asymptomatic AF recurrences by daily ECG monitoring, as compared with standard ECG and 24-h Holter recording, in patients who underwent radio frequency catheter ablation of

---

\* Corresponding Author: yccho@ikw.ac.kr

Manuscript received November. 18, 2015/ revised December 18, 2015 /accepted December. 27, 2015

1) Kyungwoon University, 1st Author

2) Keimyung University Dongsan Medical center, 2nd Author

3) Kyungwoon University, Corresponding Author

AF. A real-time, WEMS would allow not only for the detection of arrhythmia, an abrupt change in heart rhythm, but also for diagnosing ventricular tachycardia and determining the timing of treatment. The recent advancement of mobile network systems has led to the development of wireless mobile cardiac monitoring systems[4-5]. The WEMS showed usefulness in detecting cardiac arrhythmias, especially cases that are difficult to diagnose because of a rare event, baseline wander, and P wave in the presence of noise. The ECG analysis is an important method for monitoring patients. However, the ECG signal obtained for analysis is not free from noise. Diagnosing cardiac disorders and arrhythmias remain a major problem in the area of cardiac signal processing.

In this paper, we describe a patch-type ECG electrode capable of recording and analyzing continuous ECG data received from the human body. In addition, it allows the patient to continuously remotely(e.g., at home) monitor heart activity while performing daily activities. The paper describes the application of the patch-type ECG monitoring system using wireless transfer network technology[5]. An ECG signal, being intrinsically non-stationary, cannot be analyzed effectively through traditional spectral methods. Various hybrid techniques are, therefore, purposed to detect and classify cardiac arrhythmias[6-9]. Other methods have been implemented in the recent past for R-peak detection, including Fourier transform, difference operation[10], and wavelet transform methods. The difference operation method(DOM) is simple and efficient, with less computational time for QRS complex detection. It does not involve any complex mathematical calculation such as cross-correlation. In our recent study, we used the WT to develop an algorithm for ECG wave detection[11-13]. WT is a powerful

tool for the representation and analysis of ECG signal. It involves the decomposition of signal into various components[14-17]. Using the HRV analysis method[18-19], the components that are considered possible indicators of AF risk factors are statistically evaluated in terms of time and frequency domains[20-21]. Another analysis method has been used to assess the suitability of the Poincaré plot technique[22-24] for HRV analysis in subjects with AF and NSR. Previous studies found that the Poincaré plot technique is mainly characterized by simplicity, reliability, and universality.

## 2. Materials and methods

Being a non-stationary signal, the ECG has irregularities, although they may not be periodic and may show up at different intervals. Hence, clinical observation with ECG can take long hours and be very tedious. The WEMS is an available database composed of ECG recording segments from 29 NSR patients (control group) and 29 AF patients (AF group). All the AF patients(age: mean, 61.12±11.03 years; range, 40 - 89 years) and NSR patients(age: mean, 55.92±16.53 years; range, 18 - 89 years) participated in the clinical study. The algorithm was tested using ECG recordings from the cardiac patients. We obtained 24-h ECG recordings from 29 different patients with AF. The algorithm presented requires only a detection time of 5 min for a single-channel ECG. Fig. 1 shows the block diagram of the process incorporated in the proposed method. The experimental use of the wireless cardiac monitoring system and patch-type electrode is illustrated in Fig. 2.

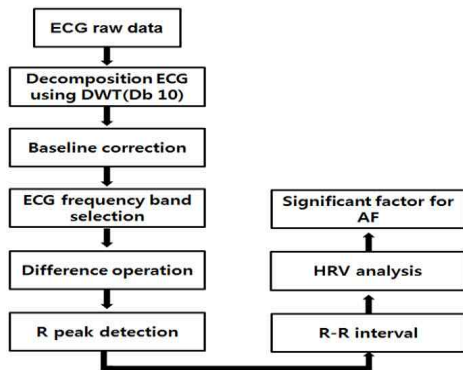


Fig. 1 Flowchart for the 1-channel ECG signal detection

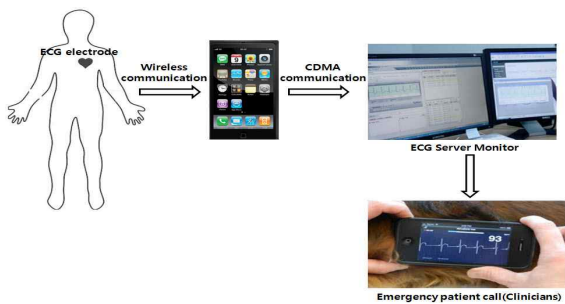


Fig. 2 Wireless cardiac monitoring system and patch-type electrode

### 2.1 Wavelet transform

The WT provides a description of a signal, decomposing it at different time-frequency resolutions. It is well suited for analysis of non-stationary signals like that in ECG. The different wave components of ECG, with its separate frequencies, become clearly visible when subjected to multi-resolution analysis. Moreover, the various noise levels, which appear at different frequency bands, and their contribution to signal distortion can be clearly identified. Selecting a wavelet function that closely matches to the morphology of the signal under investigation is of great importance in wavelet-based application. Daubechies wavelet families are similar to the shape of the QRS; hence, db8, having a morphology closely similar to that of QRS and a low-frequency

energy concentration, is being selected as the mother wavelet for the present analysis. Among many time-frequency representations, the DWT, which uses a dyadic scale is perhaps the most efficient owing to its many unique properties and its ability to solve a diverse set of problems, including data compression, biomedical signal analysis, feature extraction, noise suppression, and many more, all with a modest amount of computational expense. The DWT analyzes the signal at different resolutions through the decomposition of the signal into several successive frequency bands. It uses 2 sets of functions,  $\phi(t)$  and  $\psi(t)$ , each associated with the low- and high-pass filters, respectively.

$$\varphi(t) = \sum_n h[n]\varphi(2t - n) \tag{1}$$

$$\psi(t) = \sum_n g[n]\varphi(2t - n) \tag{2}$$

Here,  $h[n]$  and  $g[n]$  are the half-band low- and high-pass filters, respectively. A different scale and translation of their functions are key to obtaining a different frequency and time localization of the signal. Signal decomposition into different frequency bands is therefore accomplished by successive low-pass and high-pass filtering of the time domain signal. The time domain signal  $x(t)$  sampled at 300 samples forms a discrete time signal  $x[n]$ , which is first passed through a half-band high-pass filter ( $g[n]$ ) and low-pass filter ( $h[n]$ ), along with down sampling by a factor of 2.

### 2.2 Difference operation algorithm

The DOM enables simple and fast detection of QRS complexes. It essentially involves finding the difference signal or derivative. The

ECG R wave is assessed using the difference operation filter technology, and the proper threshold is determined to find the accurate ECG detection algorithm (Visual C++). In the equation,  $x[n]$  is the original ECG signal,  $0 \leq n \leq N$ , and  $N$  is the total number of signal samples. The equation is calculated as follows:  
 Step 1: Obtain the difference signal  $xd$  by Equation (3).

$$xd[n] = x[n] - x[n - 1] \quad (3)$$

Step 2: Remove the high-frequency noise signal components using a mean filter with a length of 5.

$$xF[n]=xd[n]m[n] \quad (4)$$

Step 3: Threshold  $xF[n]$  with the threshold level  $\lambda$  as follows:

$$x_T[n] = \begin{cases} x_F[n], & \text{if } x_F[n] > \lambda \\ 0, & \text{otherwise} \end{cases} \quad (5)$$

Step 4: Find the R positions from  $xT[n]$ .

The duration of each R-R interval is approximately 0.6-0.75s(182 - 227samples) at a sampling frequency of 300 Hz. The local maximum is derived from every interval starting from the  $n$  at which  $xT[n]$  is greater than 0.  $L$  is the interval length. By default,  $L$  is selected from 90 samples, which is half of the least number of samples in the R-R interval.

### 2.3 Heart rate variability

Over the past several decades, there has been a widespread interest in the study of variation in the beat-to-beat timing of the heart, known as HRV. Offline analysis of the R-R intervals uses R-peak detection algorithm.

Various analyses of the beat-to-beat variations in the R-R intervals generated HRV results in the time and frequency domains. For the time domain analysis, we calculated the mean and standard deviation values of the R-R intervals, the root mean square of the successive R-R interval differences(rMSSD), the number of R-R intervals for which successive R-R intervals differed by at least 50 ms(NN50), and the number of times successive R-R intervals differed by 50% from the index R-R interval(pNN50). The integral of the R-R density distribution divided by the maximum density distribution (R-R triangular) and the length of the base of a triangle approximating the N-N interval distribution(TINN) were also determined. Frequency domain analyses included the following: power spectral density using very low-frequency(VLF:0.003 - 0.04Hz) low frequency(LF:0.04 - 0.15Hz) and high-frequency (HF) components(0.15 - 0.40Hz), as determined by fast Fourier transform(FFT) percentages of total power in the LF and HF ranges; and the ratio of LF to HF power. All the HRV measurements were calculated for each 5-min recording segment in each patient in the NSR (control) and AF groups.

### 2.4 Poincaré plot

One simple and easy-to-comprehend nonlinear, quantitative, visual HRV analysis technique is the use of the so-called Poincaré plot. It is a graphical representation of the correlation between consecutive R-R intervals, which takes a sequence of intervals and plots each interval against the following interval. To mathematically characterize the shape of the plot, most researchers have adopted the technique of fitting an ellipse to the plot. A set of axis oriented with the line of identity is defined. The axis of the  $\Theta = \pi/4$  rad.

$$\begin{bmatrix} x_1 \\ x_2 \end{bmatrix} = \begin{bmatrix} \cos \theta & -\sin \theta \\ \sin \theta & \cos \theta \end{bmatrix} \begin{bmatrix} RR_n \\ RR_{n+1} \end{bmatrix} \quad (6)$$

In the reference system of the new axis, the dispersion of the points around the X1-axis is measured by the standard deviation denoted by SD1. This quantity measures the width of the Poincaré cloud and therefore indicates the level of short-term HRV. The length of the cloud along the line of identity measures the long-term HRV and is measured by SD2, which is the standard deviation around the X2-axis. The Poincaré plot is related to the new set of axis by a rotation. As shown in Fig. 3, the standard deviation of the distance of the points from each axis determines the width(SD1) and length(SD2) of the ellipse. The length of the current interval(RRn) is shown on the x-axis, whereas that of the post-interval is shown on the Y-axis(RRn+1). Poincare plot from with AF look very different (Fig 3(a). The contours vary: triangles, circles in various sizes, randomly distributed. The Poincare plot generated for all R-R intervals of a patient with NSR is shown in Fig 3(b).

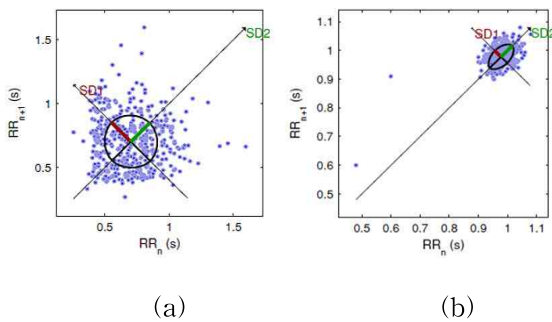


Fig. 3 The Poincaré plot with density allocation from patients with AF(Fig 3(a)). and Poincaré plot of a patient with NSR (Fig3(b)) rotated with respect to x-axis, y-axis, with its main emphasis shifted to 1(right side)

### 3. Results

ECG detection was performed using long-term real-time ECG data and the signal processing algorithm developed in our research group. The ECG records obtained from the cardiac ECG arrhythmia database(established by our research group) were sampled at 300 Hz. Figs. 4a and b show the original long-term real-time ECG from a range of 0 – 34s and wavelet decomposition. The choice of a decomposition level is dependent on the required frequency components available in the wavelet coefficient at that level. Most of the ECG energy is concentrated within the QRS complex. As shown in Fig. 4, the ECG signal energy was concentrated between 5 and 22Hz and the signal was decomposed until level 4. Using the DOM method, the R wave was detected at the location shown in Figs. 5(a) and Fig5(b) shows in differenced signal, filtered signal, threshold signal. DOM is capable of rapid calculations and detection. However, it has a signal noise detect error problem. The main advantage of the DWT is that it has a varying window size, being broad at low frequencies and narrow at high frequencies, thus leading to an optimal time-frequency resolution in all frequency ranges. Therefore, spectral analysis of the ECG signals was performed using the DWT. To evaluate the performance of the proposed DWT method, we compared the HRV signals obtained by the DOM and DWT method in the NSR and AF patients. The sensitivity and positive predictivity values are considered as the performance analysis metric of any R detection method and expressed by the following equations:

$$Sensitivity(S_c) = \frac{TP}{TP + FN} \quad (7)$$

$$Positive\ Predictivity(P) = \frac{TP}{TP + FP} \tag{8}$$

Where, TP indicates true positive(correct R peak detection); FN, false negative(undetected R peaks), and FP, false positive(misdetections). The algorithms were compared by calculating the number of TP, FN, FP values for each record. Table 1 indicates the sensitivity and positive predictivity of the detection method. We found the mean positive predictivity to be 99.88%(±0.116). The sensitivity was determined to be 99.94%(±0.116), which indicates that the method has good efficiency. A comparison of the performance of the proposed DWT algorithm with the DOM in the AF patients from the WEMS database is given in Table 2. We found that the new algorithm that we developed, the DWT method, performed better than the DOM(99.88±0.173 vs. 98.40±0.188), based on R-wave detection and analysis. The time and frequency domain measures of HRV were computed for the R-R intervals of the NSR and AF patients. The mean HRV HF and HF components indicated an inverse trend so that the means of the normalized LF component, which reflects the sympathetic nervous activity, increased in the NSR patients (45.16±18.78) but decreased in the AF patients (38.92±12.57). Correspondingly, the normalized HF obviously increased in the AF patients (61.07±12.58) and relative increased in the NSR patients(54.84±18.78), as shown in Figs. 6(a) and (b).

Statistical analysis was performed using SPSS 12.0 for Windows(SPSS Inc., Chicago, IL, USA). Univariate correlations between clinical features were evaluated using the Student t test or Mann-Whitney U test with continuous variables after checking for normality using the Kolmogorov-Smirnov test. A 2-tailed p<0.05 was considered as statistically significant. The

time domain analysis included mean R-R, STD R-R, mean HR, STD HR, RMSSD, NN50, pNN50, R-R Trian, and TNN (STD). As shown in Table 3, the STD R-R, mean HR, STD HR, RMSSD, NN50, pNN50, RR Trian, and TNN(STD) of the R-R interval series of the AF patients were significantly different from those of the control group (p<0.05). The frequency domain analysis includes VLF power(ms2), LF power (ms2), HF power(ms2), LF/HF, VLF(%), LF(%), and HF(%). The results show a significant difference in VLF

Details	Frequency range(Hz)
D1	75 - 150
D2	37.5 - 75
D3	9.375 - 18.75
D4	4.687 - 9.375
D5	2.343 - 4.687
D6	1.1718 - 2.343
D7	0.2929 - 0.5869
D8	0.1464 - 0.2929

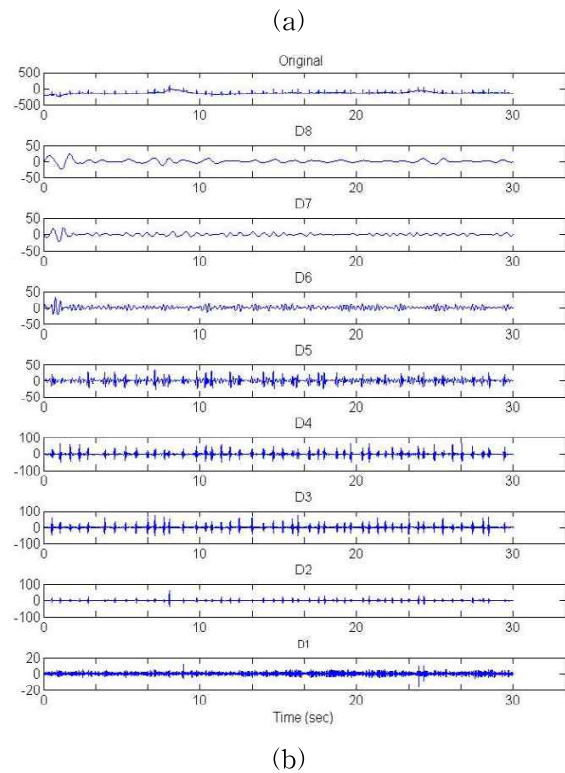


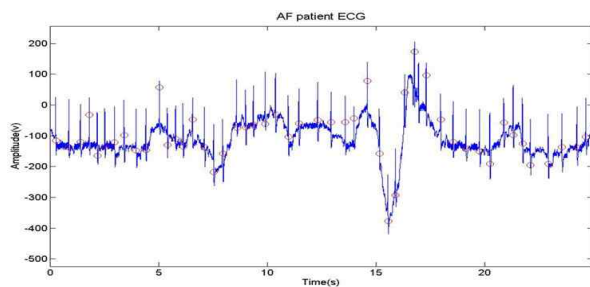
Fig. 4 Frequency band of each high pass filter range(Fig 4(a)). The DWT decomposition details by db8(Fig4 (b))

power, LF peak, HF peak, VLF(%), LF(%), and HF(%) in the control group( $p < 0.05$ ). However, no significant differences were found in VLF peak, LF peak, LF peak, HF peak, LF/HF ratio, LF(n.u), and HF(n.u). Table 3 presents the related Poincaré quantification parameters, which are dependent on the length of the R-R interval series. The parameters SD1, SD2, SD1/SD2 ratio, and interval difference have been shown for 5-min records in Table 3. Based

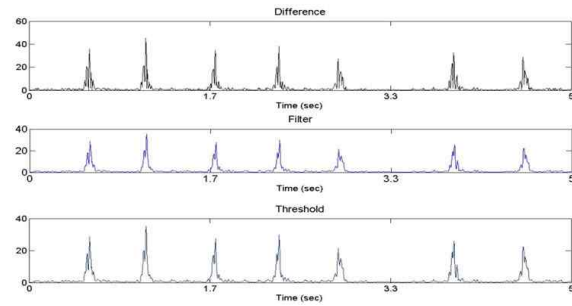
on 2D Poincare plot, the mean SD1, SD2, and SD1/SD2 values in the AF patients that indicated NSR were significantly high as follows: SD1,  $174.08 \pm 64.21$  ( $p = 0.000$ ); SD2,  $178.89 \pm 68.00$  ( $p = 0.000$ ), and SD1/SD2:  $0.98 \pm 0.17$  ( $p = 0.000$ ).

Table 1 Performance evaluation of the proposed R-wave detection method according to the detection parameters, using the arrhythmia database that we developed in our research

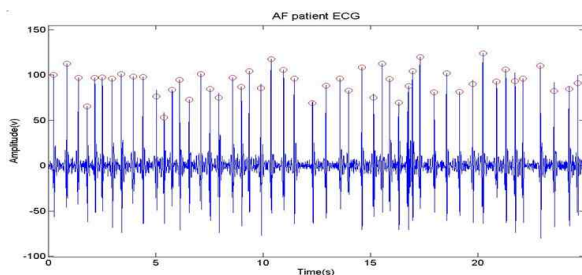
Patients	Total beats (mean)	Detected beats (mean)	TP	FN	FP	Se(%)	P (%)
KOT	608	608	608	0	0	100	100
KKJ	818	818	817	1	2	99.9	99.8
KDK	786	786	0	0	0	100	100
KST	1018	1020	1018	0	2	100	99.8
KSH	654	654	654	0	0	100	100
KSB	1222	1222	1222	0	0	100	100
KSH	800	800	800	0	0	100	100
KSW	626	628	626	0	2	100	99.7
KJB	760	760	760	0	0	100	100
KJH	1760	1765	1759	1	5	99.9	99.7
KHS	832	832	832	0	0	100	100
KHJ	1004	1004	1004	0	0	100	100
BKH	1020	1025	1018	2	3	99.8	99.7
SYJ	1250	1257	1247	3	7	99.8	99.4
SJG	866	866	866	0	0	100	100
ATS	1014	1014	1014	0	0	100	100
WJH	920	920	920	0	0	100	100
YSC	601	601	601	0	0	100	100
YYO	986	986	986	0	0	100	100
YYN	1200	1212	1195	6	6	99.5	99.5
LDS	984	987	982	3	3	99.7	99.7
LSO	892	892	892	0	0	100	100
LSJ	602	602	602	0	0	100	100
LJH	646	647	646	0	1	100	99.8
LYK	765	768	765	0	3	100	99.6
JNP	656	657	656	0	1	100	99.8
JBH	612	611	611	1	0	99.8	100
HYS	601	601	601	0	0	100	100
HHH	602	602	602	0	0	100	100
Mean						99.94( $\pm 0.116$ )	99.88( $\pm 0.173$ )



(a)



(b)



(c)

Fig. 5 The recording of the ECG signal detected using the DOM and DWT (Fig 5b shows in differenced signal, filtered signal, threshold signal and Fig 5c shows in DWT algorithm

Table 2 A comparison of the performance of the proposed DWT algorithm with the DOM in the AF patients from the WEMS database

Method	Sensitivity ( $S_e$ )	Positive Predictivity (P)
Difference Operation Method	98.97( $\pm 0.192$ )	98.40( $\pm 0.188$ )
Discrete Wavelet Transform	99.94( $\pm 0.116$ )	99.88( $\pm 0.173$ )

Table 3 Univariate analysis of the time and frequency domains for HRV. Poincaré plot technique quantification measures at 5 min

Variable	AF (n=29)	NSR (n=29)	p value
Age	61.12±11.03	55.92±16.53	0.192
Demographic			
Sex	M: 23 (79.3%) F: 6 (20.7%)	M: 17 (60.7%) F: 12 (39.3%)	0.125
Time Domain			
Mean RR (ms)	782.26±211.10	883.87±173.78	0.050 <sup>a</sup>
STD RR (ms)	181.70±64.25	64.73±32.43	0.000 <sup>b</sup>
Mean HR (1/min)	89.19±29.04	71.62±14.51	0.012 <sup>b</sup>
STD HR	29.00±22.10	8.78±6.61	0.000 <sup>b</sup>
RMSSD (STD)	249.10±93.55	63.01±40.66	0.000 <sup>b</sup>
NN50 (STD)	231.93±139.16	33.41±26.78	0.000 <sup>b</sup>
pNN50 (STD)	62.91±24.99	11.95±9.62	0.000 <sup>b</sup>
RR Trian	18.89±9.04	8.08±3.52	0.000 <sup>b</sup>
TINN (STD)	596.55±153.72	345.52±162.59	0.000 <sup>b</sup>
Frequency Domain			
VLF peak (Hz)	0.01±0.01	0.02±0.06	0.387 <sup>a</sup>
LF peak (Hz)	0.10±0.11	0.08±0.07	0.357 <sup>a</sup>
HF peak (Hz)	0.25±0.06	0.28±0.06	0.084 <sup>a</sup>
VLF power (ms <sup>2</sup> )/Hz	9485.83±19154.59	889.86±859.43	0.000 <sup>b</sup>
LF peak (ms <sup>2</sup> )/Hz	13070.45±17336.24	1002.14±1573.31	0.000 <sup>b</sup>
HF peak (ms <sup>2</sup> )/Hz	21469.28±31043.88	1851.93±3497.98	0.000 <sup>b</sup>
LF/HF	0.71±0.38	1.27±1.62	0.081 <sup>a</sup>
VLF (%)	19.64±14.17	41.21±24.23	0.001 <sup>b</sup>
LF (%)	30.42±9.27	23.96±10.61	0.006 <sup>b</sup>
HF (%)	49.93±15.73	34.83±21.19	0.007 <sup>b</sup>
LF (n.u)	38.92±12.57	45.16±18.78	0.143 <sup>a</sup>
HF (n.u)	61.07±12.58	54.84±18.78	0.144 <sup>a</sup>
Poincaré			
SD1	174.08±64.21	42.07±21.57	0.000 <sup>b</sup>
SD2	178.89±68.00	69.47±27.16	0.000 <sup>b</sup>
SD1/SD2	0.98±0.17	0.62±0.20	0.000 <sup>b</sup>
X <sub>n</sub> -X <sub>n+1</sub>	0.002±0.002	0.003±0.001	0.424 <sup>a</sup>

<sup>a</sup>Mann-Whitney U test

<sup>b</sup>Student t test

#### 4. Discussions

The ability of the WEMS to record long-term ECG data will allow clinicians to better diagnose arrhythmic events. This study demonstrated that the proposed wireless cardiac ECG system is capable of accurately detecting and analyzing AF. The proposed algorithm is simple, with low computational overhead does not involve a complex equation and has a fairly good detection sensitivity. Because these reasons, the algorithm can be easily implemented for embedded use in wireless cardiac monitoring system. Early detection is very important for providing appropriate therapeutic interventions and managing disease-related complications such as congestive heart failure and stroke.

This study demonstrated that the proposed

AF diagnose algorithm is capable of accurately detecting AF episodes and instantaneously alerting the patient and the health-care personnel, facilitating early medical intervention. Furthermore, the WEMS is superior to conventional health-care devices. It enables long-term monitoring of patients with critical conditions while they are performing daily activities. This novel system can be used for inpatients and outpatients, and it provides a long-term health monitor for healthy people. First, AF detection is based on the R-R interval variation, when the user has frequent atrial or ventricular premature beats, which can be misdiagnosed as AF. Second, in patients with AF, R-R interval variations may become too small for the system to diagnose AF accurately. Lastly, there is still considerable motion noise during the recording, which might impair diagnostic accuracy.

#### 5. Conclusions

In conclusion, this wireless cardiac ECG system is capable of early AF detection and represents a successful first step toward improving efficiency and quality of the u-health-care service. The proposed diagnose system is capable of accurately detecting AF and NSR. We found that the new algorithm that we developed, the DWT method, performed better than the DOM based on ECG detection and analysis. The statistical analysis results show a significant difference in time domain and frequency domain from those of the control group(p<0.05). Based on 2D Poincare plot, the mean SD1, SD2, and SD1/SD2 values in the AF patients that indicated NSR were significantly different from quantification parameters. Further research studies aimed at improving the hardware and software designs



of the system are necessary to enhance its efficiency and accuracy in future models.

## References

- [1] E.P. Johan, M.B. "Atrial fibrillation," *Circulation*, Vol 106, pp. 14-16, 2002.
- [2] E. Guirguis, "Holter monitoring. *Can. Fam., Physician.*, Vol 33, pp. 985-992. 1987.
- [3] G. Senatore, G. Stabile, E. Bertaglia et al., "Role of transtelephonic electrocardiographic monitoring in detecting short-term arrhythmia recurrences after radio frequency ablation in patients with atrial fibrillation," *J. Am. Coll. Cardiol.*, Vol 45, pp. 873-876, 2005.
- [4] S. S. Lobodzinski, M.M. Laks, "New devices for very long-term ECG monitoring," *Cardiol. J.*, Vol 19, pp. 210-214, 2012.
- [5] M.S. Kim, Y.C. Cho, S.T. Seo, C.S. Son, Y.N. Kim, "Auto-detection of R wave in ECG for patch type ECG remote monitoring system," *Biomed. Eng. Letter*, Vol 1, pp. 180-187, 2011.
- [6] D.A. Coast, R.M. Stern, G.G. Cano, S.A. Briller, "An approach to cardiac arrhythmia analysis using hidden Markov models," *IEEE Trans. Biomed. Eng.*, Vol 37, pp. 826-836, 1990.
- [7] Y. Ozbay, R. Ceylan, B. Karlik, "A fuzzy clustering neural network architecture for classification of ECG arrhythmias," *Comput. Biol. Med.*, Vol 36, pp. 376-388, 2003.
- [8] L. Khadra, A.S. Al-Fahoum, S. Binajaj, "A quantitative analysis approach for cardiac arrhythmia classification using higher order spectral techniques," *IEEE Trans. Biomed. Eng.*, Vol 52, pp. 1840-1845, 2005.
- [9] R. Ceylan, Y. Ozbay, "Comparison of FCM, PCA and WT techniques for classification of ECG arrhythmias using artificial neural network," *Expert Syst. Appl.*, Vol 33, pp. 286-295, 2007.
- [10] Y.C. Yeh, W. J. Wang, "QRS complexes detection for ECG signal: the difference operation method," *Comput. Methods Programs Biomed.*, Vol 91, pp. 245-254, 2008.
- [11] M.S. Kim, Y.C. Cho, S.T. Seo, C.S. Son, Y.N. Kim, "A new method of ECG feature detection based on combined wavelet transform for u-health service," *Biomed. Eng. Letter*, Vol 1, pp. 67-76, 2011.
- [12] Y.C. Cho, M.S. Kim, J.O. Yoon, "Comparison of Characteristics of P-Wave Detection in ECG with Wireless Patch Electrodes," *Journal of the Korea Industrial Information System Society*, Vol 19, pp.43-52, 2014.
- [13] Y.S. Heo, J.C. Lee and Y.N. Kim, "Analysis and Processing of Driver's Biological Signal of Workload," *Journal of the Korea Industrial Information System Society*, Vol 20, pp. 87-93, 2015.
- [14] S. Mallet, "A theory for multiresolution signal decomposition: the wavelet representation," *IEEE Trans. Pattern Anal. Mach. Intelligence*, Vol 11, pp.674-693. 1989.
- [15] A. Grap, "An introduction to wavelets," *IEEE Comput. Sci. Eng.*, Vol 2, 1995.
- [16] S.Z. Mahamoodibad, A. Ahmadian, M.D. Abolhasani, "ECG feature extraction using Daubechies wavelets, Proceedings of Fifth IASTED International Conference., pp. 343-348, 2005.
- [17] I. Daubechies, "The wavelet transform, time-frequency localization and signal analysis," *IEEE Trans. Inform. Theory*, Vol 36, pp. 961-1005, 1990.
- [18] M. Malik, A.J. Camm, "(Eds.), Heart rate variability," Futura Pub. Co. Inc., Armonk, New York. 1995.
- [19] R.E. Kleiger, P.K. Stein, M.S. Bosner, J.N.

Rottman, "Time domain measurements of heart rate variability," in: M. Malik., A.J. Camm (Eds.), Heart rate variability, Futura Pub. Co. Inc., Armonk, New York, pp. 33-45, 1995.

- [20] S. Akselrod, D. Gordon, F.A. Ubel, D.C. Shannon, A.C. Barger, R.I. Cohen, "Power spectrum analysis of heart rate fluctuation: a quantitative probe of beat-to-beat cardiovascular control," Science, Vol 213, pp. 220-222, 1981.
- [21] N.S. Cai, M. Dohnal, S.B. Olsson, "Methodological aspects of the use of heart rate stratified R-R interval histograms in the analysis of atrioventricular conduction during atrial fibrillation," Cardiovasc. Research., Vol 21, pp. 455-462, 1987.
- [22] M. Brennan, M. Palaniswami, P. Kamen, "Do existing measures of Poincaré plot geometry reflect nonlinear features of heart rate variability?," IEEE Trans. BME., Vol 48, pp. 1342-1347, 2001.
- [23] D. Singh, K. Vinod, "Effect of R-R segment duration on short-term HRV assessment using Poincare plot," Proceeding of ICISIP, 2005.
- [24] T. Thong, "Geometric measures of Poincare plots for the detection of small sympathovagal shifts," Proceedings of the 29th Annual International Conference of the IEEE EMBS, France., pp. 23-26, 2007.



**김민수 (Min Soo Kim)**

- 정회원
- 경일대학교 전기공학과 공학사
- 영남대학교 전기공학과 공학석사
- 영남대학교 전자공학과 공학박사
- 토요하시기술과학대학 박사후 연구원
- 경운대학교 항공대학 항공정보통신공학과 교수
- 관심분야 : 생체임피던스, 생체신호처리



**김윤년 (Yoon Nyun Kim)**

- 정회원
- 경북대학교 의과대학 의학사
- 경북대학교 의과대학 의학석사
- 경북대학교 의과대학 의학박사
- 계명대학교 의과대학 내과학교실(심장내과)교수
- 관심분야 : 부정맥, 전기생리적검사, 도자절제술, 영구심박동기, 중재시술, 고혈압, 심부전



**조영창 (Young Chang Cho)**

- 정회원
- 영남대학교 전기공학과 공학사
- 영남대학교 전자공학과 공학석사
- 영남대학교 전자공학과 공학 박사
- 경운대학교 항공대학 항공정보통신공학과 교수
- 관심분야 : DSP, 영상신호처리